Journal of Sound and Vibration (1997) **200**(4), 505–518

THREE-DIMENSIONAL VIBRATION ANALYSIS OF SOLID CYLINDERS OF POLYGONAL CROSS-SECTION USING THE *p*-RITZ METHOD

K. M. Liew, K. C. Hung and M. K. Lim

Division of Engineering Mechanics, School of Mechanical and Production Engineering, Nanyang Technological University, Nanyang Avenue, Singapore 639798

(*Received* 4 *July* 1994, *and in final form* 14 *August* 1996)

Theoretical and numerical analyses and some observations on the physical phenomena of free vibration of solid cylinders having square and hexagonal cross-sections with combinations of fixed and free ends are reported. The formulation is established based on the linear, small-strain, three-dimensional elasticity principle, and the *p*-Ritz method is employed for computing the solution of the problem. By expanding the displacements in spatial co-ordinates, integral expressions for strain and kinetic energies in a three-dimensional setting are derived in Cartesian form. Sets of one- and two-dimensional orthogonal polynomials are constructed to represent the three-dimensional variations in the longitudinal and lateral surface directions. A basic function is introduced in these polynomials to cater for the stress free lateral surfaces and the kinematic constraints at both ends. Several examples are solved to demonstrate the applicability of the method. First known results in terms of vibration frequency parameters and mode shapes of cylinders having square and hexagonal cross-sections for various symmetry classes and end constraints are presented and the physics behind the results is highlighted. These new results may serve as benchmark data for future research development in simplified beam theories.

1. INTRODUCTION

The mathematical and computational complexities in three-dimensional modelling of solid cylinders of polygonal cross-section have led to the development of simple refined beam theories [1, 2]. It is well known that certain limitations exist in any simplified beam theories; therefore, an exact three-dimensional solution of this problem is always necessary for checking and defining the limitations and accuracies of these theories.

Contemporary engineering practice demands highly accurate engineering prediction of the dynamic behaviour of high speed mechanisms. This replaces the use of unrealistic safety factors. The most direct approach to accurate frequency solutions, however, is to base the analysis on exact three-dimensional linear elasticity theory. This is more attainable nowadays due to the rapid advancement in computer hardware technology. Researchers have at their disposal a much wider array of mathematical tools and numerical processors for developing computational models that are closer to the true dynamic behaviour of structures in three dimensions. The aim of this study is to develop one such model specifically for the accurate vibration study of solid cylinders with polygonal cross-sections.

Several researchers have attempted to provide frequency results based on the three-dimensional elasticity approach. Different types of series functions have also been proposed to approximate the displacement variations in three dimensions. Hutchinson [3] proposed a formulation that works well with the Bessel series function for the analysis of stress free circular cylinders. His work was further extended to study the free vibration of

0022–460X/97/090505 + 14 $25.00/0/sv960715

rectangular parallelepipeds and beams of rectangular cross-section [4, 5]. Simple polynomial functions have been employed by Leissa and Zhang [6] to analyze the three-dimensional vibration of cantilevered parallelepipeds. The simple polynomials used in their analysis were constructed specifically to satisfy only the cantilevered boundaries of the rectangular elastic solid. These series functions have proven to be effective for the specific purpose; however, extrapolation to more general cases may not be feasible. To make possible the analysis of a wider class of three-dimensional elastic solids, it is imperative to devise displacement functions that can efficiently accommodate the geometric complexity of the three-dimensional analysis [7–10]. It is toward this end that the current research is initiated.

In this paper, the detailed formulation of the three-dimensional linear elasticity solutions for the free vibration of elastic solid cylinders of polygonal cross-section is discussed. In the numerical implementation, the *p*-Ritz method [7–10] is employed, in which the polynomial-based displacement functions are uniquely constructed from sets of one- and two-dimensional orthogonal polynomials. The one-dimensional polynomial expansion approximates the displacement variations in the longitudinal direction [7]. The two-dimensional polynomial series, on the other hand, represents the lateral surface variations of the elastic cylinder in the Cartesian frame [8–10]. Basic functions are introduced in these polynomials with which to account for the stress free lateral surfaces and to satisfy the kinematic constraints at both ends of the elastic cylinders. The accuracy of these polynomials in the present three-dimensional *p*-Ritz formulation is established through convergence and comparison studies.

The primary objectives of this paper are (1) to present a detailed formulation of the polynomial-based, three-dimensional, linear elastic solution approach for free vibration problems, (2) to supplement the existing literature with new free vibration data of elastic solid cylinders, and (3) to provide possible benchmarking reference for research development in simplified beam theories.

2. MATHEMATICAL FORMULATION

2.1. PRELIMINARY DEFINITION

The geometric configuration of a solid cylinder of polygonal shape, as shown in Figure 1, is defined in a right-handed Cartesian co-ordinated system (x_1, x_2, x_3). The cross-section of the cylinder is denoted by a in the x_1 direction and b in the x_2 direction. The cylinder is of finite length L. In general, the spatial displacement field is resolved into u_1, u_2 in the lateral direction and u_3 in the longitudinal direction, respectively. The energy functional is expressed in terms of u_1, u_2 and u_3 components. The aim of this study is to determine the vibration frequencies and three-dimensional displacement mode shapes of cylinders with combinations of free and clamped (fixed) ends.

2.2. FORMULATION OF ENERGY FUNCTIONAL

With $\varepsilon = \{\varepsilon_{ij}\}$, $i, j = 1, 2, 3$ and $\sigma = \{\sigma_{ij}\}$, $i, j = 1, 2, 3$ denoting the strain and stress tensors, the strain energy, $\mathscr{U}$, can be expressed as

$$\mathscr{U} = \frac{1}{2}\iiint_V \sigma^{\mathrm{T}}\varepsilon \, \mathrm{d}V \tag{1}$$

where the integration is performed over the volume of cylinder.

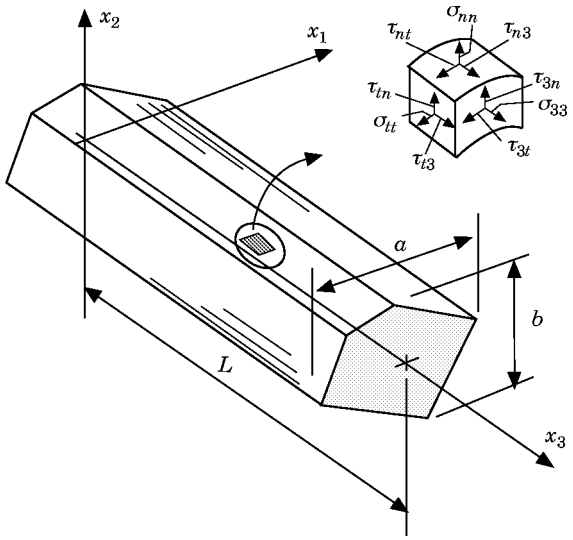

Figure 1. Geometry and dimensions of an elastic solid polygonal cylinder.

The constitutive relationship between the stress and strain is given by

$$\sigma = \mathbf{D}\varepsilon \tag{2}$$

in which **D** is the compliance matrix.

For a three-dimensional transversely isotropic elastic solid, equation (2) can be written in full as

$$\begin{Bmatrix} \sigma_{11} \\ \sigma_{22} \\ \sigma_{33} \\ \sigma_{12} \\ \sigma_{23} \\ \sigma_{13} \end{Bmatrix} = \begin{bmatrix} d_{11} & d_{12} & d_{13} & 0 & 0 & 0 \\ & d_{22} & d_{26} & 0 & 0 & 0 \\ & & d_{33} & 0 & 0 & 0 \\ & & & d_{44} & 0 & 0 \\ & \text{Sym} & & & d_{55} & 0 \\ & & & & & d_{66} \end{bmatrix} \begin{Bmatrix} \varepsilon_{11} \\ \varepsilon_{22} \\ \varepsilon_{33} \\ \varepsilon_{12} \\ \varepsilon_{23} \\ \varepsilon_{13} \end{Bmatrix}, \tag{3}$$

where σ_{ii}, $i = 1, 2, 3$ are the normal stresses, σ_{12}, σ_{23}, σ_{13} are the tangential stresses and ε_{ij} are the corresponding strain components.

For isotropic materials, the components d_{ij} are given by

$$d_{ii} = \gamma + 2G,\ i = 1, 2, 3, \qquad d_{12} = d_{13} = d_{23} = \gamma, \qquad d_{ii} = 2G,\ i = 4, 5, 6, \tag{4a–c}$$

where the Lamé constant γ and shear modulus G are defined as

$$\gamma = vE/[(1 + v)(1 - 2v)], \qquad G = E/2(1 + v), \tag{5a,b}$$

in which E is the modulus of elasticity and v is the Poisson ratio.

In general, the linear strain components can be defined as

$$\varepsilon_{ii} = \partial u_i/\partial x_i,\ i = 1, 2, 3, \qquad \varepsilon_{1i} = \partial u_1/\partial x_i + \partial u_i/\partial x_1,\ i = 2, 3, \qquad \varepsilon_{23} = \partial u_2/\partial x_3 + \partial u_3/\partial x_2. \tag{6a–c}$$

Upon substituting equations (2)–(6) into equation (1), the strain energy becomes

$$\mathscr{U} = \frac{1}{2}\iiint_V \left\{\gamma\left(\sum_{i=1}^{3} u_{i,i}\right)^2 + 2G\left(\sum_{i=1}^{3} u_{i,i}^2\right) + G[(u_{1,2}+u_{2,1})^2 + (u_{2,3}+u_{3,2})^2 + (u_{1,3}+u_{3,1})^2]\right\} \mathrm{d}V, \tag{7}$$

in which the comma denotes partial differentiation.

The kinetic energy for the solid cylinder can be expressed as

$$\mathscr{T} = \frac{\rho}{2}\iiint_V \left\{\left(\frac{\partial u_1}{\partial t}\right)^2 + \left(\frac{\partial u_2}{\partial t}\right)^2 + \left(\frac{\partial u_3}{\partial t}\right)^2\right\} \mathrm{d}V, \tag{8}$$

where ρ is the mass per unit volume.

The periodic displacement components, for simple harmonic motion, can be expressed in term of displacement amplitude functions,

$$u_i = U_i(x_1, x_2, x_3)\, \mathrm{e}^{\mathrm{i}\omega t}, \qquad i = 1, 2, 3 \tag{9}$$

where ω is the angular frequency of vibration.

The maximum strain energy $\mathscr{U}_{\max}$ and kinetic energy $\mathscr{T}_{\max}$ of the solid cylinder are obtained from equations (7)–(9) by eliminating the periodic elements and replacing the displacement components by the corresponding amplitude functions.

3. METHOD OF SOLUTION

3.1. ADMISSIBLE DISPLACEMENT FUNCTIONS

The assumed spatial displacement field is based on a separate assumption for the $U_i(x_1, x_2, x_3)$, and each of them is expressed as a summation of a series of terms which are products of one-dimensional functions $\psi_n(x_3)$ in the longitudinal direction and two-dimensional functions $\phi_m(x_1, x_2)$ for the cross-section. The displacement field is therefore given by

$$U_i(x_1, x_2, x_3) = \sum_{m=1}^{M}\sum_{n=1}^{N} c_{mn}^{i}\, {}^{i}\phi_m(x_1, x_2)\, {}^{i}\psi_n(x_3), \qquad i = 1, 2, 3, \tag{10}$$

where c_{mn}^{i} are the unknown coefficients.

The one-dimensional longitudinal function $\psi_n(x_3)$ is generated orthogonally through a recurrence process [7].

For $\Psi_k(x_3) \in \{{}^{i}\psi_k(x_3),\ i = 1, 2, 3\}$, the orthogonalization process gives

$$\Psi_{k+1}(x_3) = \{f(x_3) - \Xi_k^1\}\Psi_k(x_3) - \Xi_k^2 \Psi_{k-1}(x_3), \qquad k = 1, 2, 3, \ldots, \tag{11}$$

where

$$\Xi_i^1 = {}_1\Delta_k / {}_2\Delta_k, \qquad \Xi_i^2 = {}_2\Delta_k / {}_3\Delta_{k-1}, \tag{12a}$$

$${}_1\Delta_k = \int_{-L/2}^{L/2} f(x_3)\Psi_k^2(x_3)\,\mathrm{d}x_3, \qquad {}_2\Delta_k = \int_{-L/2}^{L/2} \Psi_k^2(x_3)\,\mathrm{d}x_3,$$

$${}_3\Delta_{k-1} = \int_{-L/2}^{L/2} \Psi_{k-1}^2(x_3)\,\mathrm{d}x_3, \tag{12b–d}$$

in which $\Psi_0(x_3) = 0$ and $f(x_3)$ is the generating function that can be arbitrary chosen but with the higher polynomial series satisfies the essential geometric boundary conditions.

It should be noted that the functions generated satisfy the orthogonality condition

$$\int_{-L/2}^{L/2} \Psi_m(x_3)\Psi_n(x_3)\,\mathrm{d}x_3 = n_{ij}\,\delta_{ij}, \tag{13}$$

where δ_{ij} is the Kronecker delta and the values of n_{ij} are assigned during the normalization process.

The two-dimensional cross-sectional function $\phi_m(x_1, x_2)$ is generated through a recursive relation. The function is formed of the product of a two-dimensional polynomial space and a basic function [8–10]. The details are as follows.

For $\Phi_k(x_1, x_2) \in \{{}^i\phi_k(x_1, x_2);\ i = 1, 2, 3\}$, the recurrence process gives

$$\Phi_k(x_1, x_2) = g_k(x_1, x_2)\Phi_1(x_1, x_2) - \sum_{j=1}^{k-1} \Theta_{jk}\Phi_j(x_1, x_2), \tag{14}$$

where

$$\Theta_{jk} = {}_1\otimes_{jk} / {}_2\otimes_j, \tag{15a}$$

$${}_1\otimes_{jk} = \iint_A g_k(x_1, x_2)\Phi_1(x_1, x_2)\Phi_j(x_1, x_2)\,\mathrm{d}x_1\,\mathrm{d}x_2, \tag{15b}$$

$${}_2\otimes_j = \iint_A \Phi_j^2(x_1, x_2)\,\mathrm{d}x_1\,\mathrm{d}x_2, \tag{15c}$$

in which the limit of the double integral, A, represents the surface area of the cross-section of the cylinder.

The generating functions are generated according to the procedure

$$\sum_{k=1}^{m} g_k(x_1, x_2) = \sum_{q=0}^{p}\sum_{l=0}^{q} x_1^{2(q-l)}x_2^{2l}, \tag{16}$$

in which the total number of terms, m is related to p by

$$m = (p + 1)(p + 2)/2. \tag{17}$$

Similarly the two-dimensional functions satisfy the orthogonality condition

$$\iint_A \Phi_m(x_1, x_2)\Phi_n(x_1, x_2)\,\mathrm{d}x_1\,\mathrm{d}x_2 = n_{ij}\,\delta_{ij}, \tag{18}$$

where δ_{ij} and n_{ij} have been defined earlier.

In the above formulation, two basic (starting) functions are needed. One is for the longitudinal direction and the other for the cross-section surfaces. These functions are generated to satisfy the essential boundary conditions.

The geometric and natural boundary conditions of the ends of the cylinder are (1) stress free, $\sigma_{13} = \sigma_{23} = \sigma_{33} = 0$ (no geometric boundary condition), and (2) clamped (fixed), $u_1 = u_2 = u_3 = 0$ (only geometric boundary conditions). Now a basic function is constructed to satisfy only the geometric boundary conditions (since they are the only criteria of the Ritz method). Therefore the basic function in the longitudinal direction is constructed by the products of the respective boundary equation at each end,

$$\psi_{\alpha 1}(x_3) = (x_3 - L/2)^{\odot_{\alpha 1}}(x_3 + L/2)^{\odot_{\alpha 2}}, \tag{19}$$

in which for the in-plane directions (U_1 and U_2), the value of $\odot$ takes on 0 for stress free, and 1 for clamped (fixed). However, for the longitudinal direction (U_3), $\odot$ takes on 0 for stress free, and 1 for clamped (fixed) ends.

The basic function for the cross-section must satisfy the stress free conditions at the lateral surfaces: $\sigma_{nn} = \sigma_{nt} = \sigma_{n3} = 0$. For a symmetric cylinder, the modes can be classified into four symmetry classes: double-symmetry (SS), symmetry–antisymmetry (SA), antisymmetry–symmetry (AS), and double-antisymmetry (AA), about the x_1x_3- and x_2x_3-planes, respectively.

The basic functions that satisfy the essential geometric boundary conditions of different symmetry classes are as follows: (a) for the double-symmetry mode (SS), ${}^i\phi_1(x_1, x_2)$ are given by

$${}^1\phi_1(x_1, x_2) = x_1, \qquad {}^2\phi_2(x_1, x_2) = x_2, \qquad {}^3\phi_1(x_1, x_2) = 1; \tag{20a–c}$$

(b) for the symmetry–antisymmetry mode (AS), ${}^i\phi_1(x_1, x_2)$ are given by

$${}^1\phi_1(x_1, x_2) = x_1x_2, \qquad {}^2\phi_1(x_1, x_2) = 1, \qquad {}^3\phi_1(x_1, x_2) = x_2; \tag{21a–c}$$

(c) for the antisymmetry–symmetry mode (SA), ${}^i\phi_1(x_1, x_2)$ are given by

$${}^1\phi_1(x_1, x_2) = 1, \qquad {}^2\phi_1(x_1, x_2) = x_1x_2, \qquad {}^3\phi_1(x_1, x_2) = x_1; \tag{22a–c}$$

(d) for the double-antisymmetry mode (AA), ${}^i\phi_1(x_1, x_2)$ are given by

$${}^1\phi_1(x_1, x_2) = x_2, \qquad {}^2\phi_1(x_1, x_2) = x_1, \qquad {}^3\phi_1(x_1, x_2) = x_1x_2. \tag{23a–c}$$

3.2. GOVERNING EIGENVALUE EQUATION

The energy functional, $\mathscr{U}_{\max} - \mathscr{T}_{\max}$, expressed in terms of the polynomial functions is now minimized with respect to the unknown coefficients,

$$(\partial/\partial c_{ij}^{\alpha})\{\mathscr{U}_{\max} - \mathscr{T}_{\max}\} = 0, \qquad \alpha = 1, 2, 3, \tag{24}$$

which leads to the governing eigenvalue equation

$$(\mathbf{K} - \lambda^2\mathbf{M})\{\mathbf{c}\} = \{\mathbf{0}\}, \tag{25}$$

where

$$\mathbf{K} = \begin{bmatrix} \mathbf{k}^{11} & \mathbf{k}^{12} & \mathbf{k}^{13} \\ & \mathbf{k}^{22} & \mathbf{k}^{23} \\ \text{sym} & & \mathbf{k}^{33} \end{bmatrix}, \qquad \mathbf{M} = \begin{bmatrix} \mathbf{m}^{11} & \mathbf{0} & \mathbf{0} \\ & \mathbf{m}^{22} & \mathbf{0} \\ \text{sym} & & \mathbf{m}^{33} \end{bmatrix}, \tag{26, 27}$$

and $\{\mathbf{c}\} = \{c_{ij}^1, c_{ij}^2, c_{ij}^3\}^{\mathrm{T}}$ is the column vector of the unknown coefficients.

The elements in the stiffness matrix $\mathbf{k}^{\alpha\beta}$ are given by

$$k_{minj}^{11} = (\Lambda_1/\Lambda_2)(\mathscr{E}_{mi}^{1010}\mathscr{F}_{nj}^{00})_{11} + \tfrac{1}{2}(\mathscr{E}_{mi}^{0100}\mathscr{F}_{nj}^{00})_{11} + \tfrac{1}{2}[a/L]^2(\mathscr{E}_{mi}^{0000}\mathscr{F}_{nj}^{11})_{11}, \tag{28a}$$

$$k_{minj}^{12} = (\nu/\Lambda_2)(\mathscr{E}_{mi}^{1001}\mathscr{F}_{nj}^{00})_{12} + \tfrac{1}{2}(\mathscr{E}_{mi}^{0110}\mathscr{F}_{nj}^{00})_{12} \tag{28b}$$

$$k_{minj}^{13} = [a/L]\{(\nu/\Lambda_2)(\mathscr{E}_{mi}^{1000}\mathscr{F}_{nj}^{01})_{13} + \tfrac{1}{2}(\mathscr{E}_{mi}^{0010}\mathscr{F}_{nj}^{10})_{13}\}, \tag{28c}$$

$$k_{minj}^{22} = (\Lambda_1/\Lambda_2)(\mathscr{E}_{mi}^{0101}\mathscr{F}_{nj}^{00})_{22} + \tfrac{1}{2}(\mathscr{E}_{mi}^{1010}\mathscr{F}_{nj}^{00})_{22} + \tfrac{1}{2}[a/L]^2(\mathscr{E}_{mi}^{0000}\mathscr{F}_{nj}^{11})_{22}, \tag{28d}$$

$$k_{minj}^{23} = [a/L]\{(\nu/\Lambda_2)(\mathscr{E}_{mi}^{0010}\mathscr{F}_{nj}^{01})_{23} + \tfrac{1}{2}(\mathscr{E}_{mi}^{0001}\mathscr{F}_{nj}^{10})_{23}\}, \tag{28e}$$

$$k_{minj}^{33} = [a/L]^2\{(\Lambda_1/\Lambda_2)(\mathscr{E}_{mi}^{0000}\mathscr{F}_{nj}^{00})_{33} + \tfrac{1}{2}(\mathscr{E}_{mi}^{0101}\mathscr{F}_{nj}^{00})_{33}\} + \tfrac{1}{2}(\mathscr{E}_{mi}^{0101}\mathscr{F}_{nj}^{00})_{33}, \tag{28f}$$

and the elements for the mass matrix $\mathbf{m}^{\alpha\beta}$ are given by

$$m_{minj}^{11} = \Lambda_3\{\mathscr{E}_{mi}^{0000}\mathscr{F}_{nj}^{00}\}_{11}, \qquad m_{minj}^{22} = \Lambda_3\{\mathscr{E}_{mi}^{0000}\mathscr{F}_{nj}^{00}\}_{22}, \qquad m_{minj}^{22} = \Lambda_3\{\mathscr{E}_{mi}^{0000}\mathscr{F}_{nj}^{00}\}_{33}, \tag{29a–c}$$

where the product of integrals in equations (28) and (29) are defined as

$$\{\mathscr{E}_{mi}^{\mathrm{defg}}\}_{\alpha\beta} = \int\int_{\bar{A}}\left[\frac{\partial^{d+e}\{^{\alpha}\phi_m(\bar{x}_1, \bar{x}_2)\}}{\partial\bar{x}_1^d\,\partial\bar{x}_2^e}\right]\left[\frac{\partial^{f+g}\{^{\beta}\phi_i(\bar{x}_1, \bar{x}_2)\}}{\partial\bar{x}_1^f\,\partial\bar{x}_2^g}\right]\mathrm{d}\bar{x}_1\,\mathrm{d}\bar{x}_2, \tag{30a}$$

$$\{\mathscr{F}_{nj}^{rs}\}_{\alpha\beta} = \int_{-1/2}^{1/2}\left[\frac{\partial^r\{^{\alpha}\psi_n(\bar{x}_3)\}}{\partial\bar{x}_3^r}\right]\left[\frac{\partial^s\{^{\beta}\psi_j(\bar{x}_3)\}}{\partial\bar{x}_3^s}\right]\mathrm{d}\bar{x}_3, \tag{30b}$$

in which $\Lambda_1 = 1 - \nu$, $\Lambda_2 = 1 - 2\nu$, and $\Lambda_3 = 1 + \nu$. The normalized variables, $\bar{x}_1$, $\bar{x}_2$ and $\bar{x}_3$, are defined as

$$\bar{x}_1 = x_1/a, \qquad \bar{x}_2 = x_2/b, \qquad \bar{x}_3 = x_3/L. \tag{31}$$

With the establishment of the stiffness **K** and mass **M** matrices, the frequency parameters and mode shapes can be obtained by solving a standard eigenvalue problem through the QR algorithm. The frequency parameters λ are related to the natural frequencies ω by

$$\lambda = \omega a\sqrt{\rho/E}. \tag{32}$$

4. RESULTS AND DISCUSSION

The above procedures have been written into a FORTRAN programme which is used to determine the non-dimensional frequency parameter, λ, and vibration mode shapes of elastic cylinders with square and hexagonal cross-sections subject to different constraints at the ends. In the following study, the symbols, *F*, and *C* denote free, and clamped (fixed) conditions at the ends, respectively.

4.1. CONVERGENCE AND COMPARISON STUDIES

Table 1 shows the rate of convergence of the frequency parameter, λ, for a cylinder of square cross-section. From the symmetry inherent in the geometry, the vibration mode shapes are conveniently classified into double-symmetry (SS), symmetry–antisymmetry (SA), antisymmetry–symmetry (AS), and double-antisymmetry (AA) modes about the planes, $x_1\ x_3$ and $x_2\ x_3$. This symmetry classification has significantly reduced the determinant size of the eigenvalue matrix and leads to better computational efficiency. The order, p, of the two-dimensional polynomial and the number of terms, q, of the one-dimensional polynomial are varied in different steps to demonstrate the relative effect on the overall convergence behaviours of the present method. Generally it is observed that the Ritz method tends to over-estimate the natural frequencies of the cylinders. As more and more terms are taken in the polynomial functions for the displacement function, the accuracy improves and the results converge monotonically to an acceptable frequency solution. It is found that satisfactory converged solutions to four significant figures are attainable with $p = 5$ and $q = 8$ for most modes of interest.

For an elastic solid cylinder with a square cross-section, comparison is made between the present solutions and that of Leissa and Zhang [6]. In the latter, the vibration frequency of the cantilevered square cylinder is computed from a Ritz energy approach with simple polynomial shape functions. Table 2 presents the comparison study of the first five modes at each symmetry class of vibration calculated from both approaches. The percentage discrepancies are in the range of 0·1% to 9·0%. The first two lowest modes are found to be well within 1·0%. The maximum difference is registered at higher modes with a percentage discrepancy of 9·0% with the present solutions being lower. A detailed study of the convergence table in the reference reveals that the number of terms employed does not ensure sufficiently converged results for the higher modes. This fact may account for

TABLE 1

Convergence of frequency parameters, $\lambda = \omega a\sqrt{\rho/E}$, *for a free-free cylinder with square cross-section* ($a/b = 1{\cdot}0$, $L/a = 2{\cdot}0$ *and* $\nu = 0{\cdot}3$)

Orders of polynomials		Mode sequence number				
p	q	1	2	3	4	5
			(a) SS mode			
5	5	1·53723	2·48768	2·57564	2·75548	2·75549
6	5	1·53722	2·48764	2·57563	2·75546	2·75546
5	6	1·53722	2·48761	2·57561	2·75543	2·75543
5	7	1·53721	2·48760	2·57561	2·75541	2·75541
5	8	1·53721	2·48760	2·57560	2·75539	2·75539
			(b) SA mode			
5	5	1·02144	1·70719	2·42924	2·45019	2·73797
6	5	1·02142	1·70716	2·42921	2·45017	2·73794
5	6	1·02141	1·70714	2·42920	2·45013	2·73793
5	7	1·02140	1·70712	2·42919	2·45011	2·73789
5	8	1·02140	1·70712	2·42919	2·45011	2·73789
			(c) AA mode			
5	5	0·89354	1·77936	2·04725	2·13129	2·44497
6	5	0·89352	1·77933	2·04724	2·13126	2·44494
5	6	0·89351	1·77930	2·04721	2·13125	2·44492
5	7	0·89351	1·77929	2·04720	2·13122	2·44490
5	8	0·89351	1·77929	2·04720	2·13121	2·44489

TABLE 2

Comparison of frequency parameters, $\lambda = \omega a\sqrt{\rho/E}$, for cantilevered elastic solid cylinder of square cross-section with length-to-width ratio $L/a = 2{\cdot}0$

Symmetry classes	Source of results	Mode sequence number 1	2	3	4	5
SS mode	Leissa and Zhang [6]	0·79690	2·2906	2·5323	2·7480	2·9305
	Present 3D solution	0·79422	2·2743	2·5260	2·7425	2·8578
		(−0·337)†	(−0·717)	(−0·249)	(−0·201)	(−2·54)
SA mode	Leissa and Zhang [6]	0·22186	0·83555	1·8619	2·3138	2·7160
	Present 3D solution	0·22007	0·83061	1·7314	2·2214	2·6421
		(−0·813)	(−0·595)	(−7·53)	(−4·16)	(−2·80)
AA mode	Leissa and Zhang [6]	0·45202	1·3596	2·0894	2·4429	2·4719
	Present 3D solution	0·45092	1·3502	2·0855	2·2414	2·4697
		(−0·244)	(−0·696)	(−0·187)	(−8·99)	(−0·089)

† Figures in parenthesis denote the discrepancies in %.

the significant discrepancy between the present solutions and those values of Leissa and Zhang [6] at the higher modes.

To facilitate a comparison with the work of Hutchinson and Zillmer [4], the frequency parameters from different sources are plotted in Figure 2 for a/b ratios varying from 0·2 to 0·5. The comparison has shown that the present predictions and those of Hutchinson and Zillmer [4] for a free–free square beam are found to be in close agreement.

4.2. PARAMETRIC STUDIES

After having established the numerical convergence and accuracy of the three-dimensional p-Ritz model, sets of frequency results and mode shape plots were computed. The vibration characteristics of elastic solid cylinders of each symmetry class can be

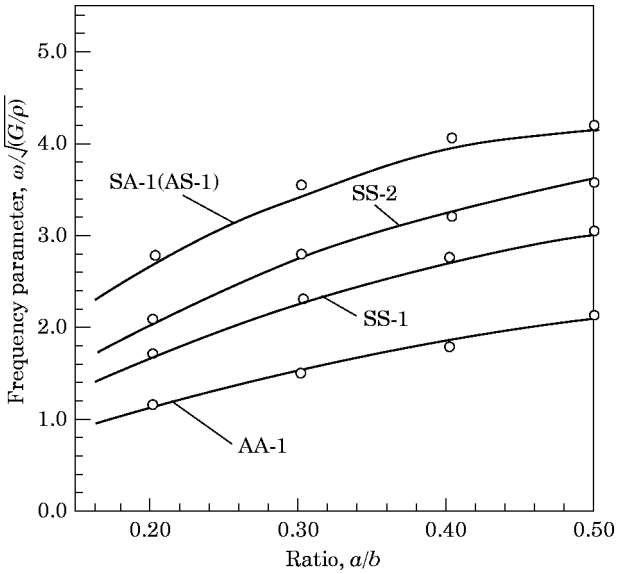

Figure 2. Comparison of frequency parameters for a free–free square cylinder. ○, Hutchinson and Zillmer [4]; ——, present 3D analysis.

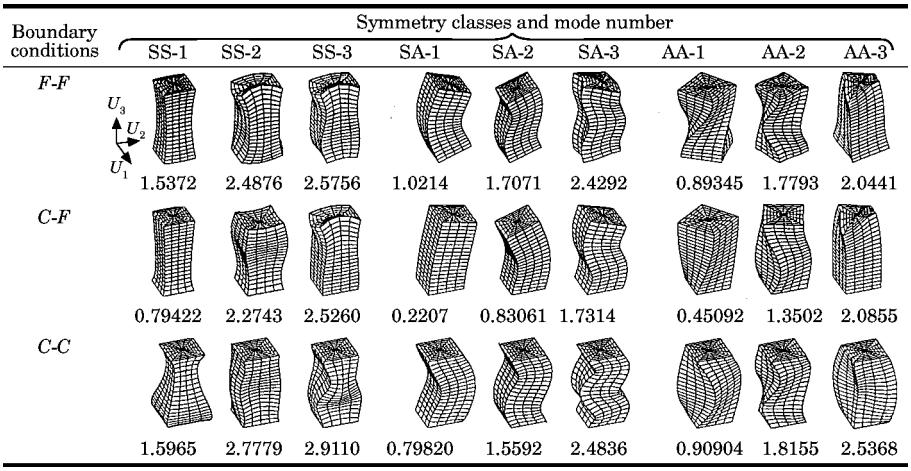

Figure 3. Vibration mode shapes of square cylinders subjected to different end support conditions ($a/b = 1{\cdot}0$, $L/a = 2{\cdot}0$, $\nu = 0{\cdot}3$, $\lambda = \omega a\sqrt{\rho/E}$).

clarified by considering the respective deformed mode shapes. Figures 3 and 4 depict the corresponding deformed mode shape plots of cylinders with square and hexagonal cross-sections. Each figure demonstrates the influence of boundary constraints at both ends for the mode of vibration. From these figures, the following remarks can be made.

It is observed that the fundamental modes of the distinct symmetry classes, namely the SS-1, SA-1, AS-1 and AA-1 modes, are exhibiting axial extensional, transverse bending about x_1, transverse bending about x_2 and axial torsional motions, respectively. A cross-examination of these figures further reveals the interesting fact that the cross-sectional geometries of the polygonal cylinder do not have a significant effect on the fundamental vibration mode shapes. However, for the cylinder with a square cross-section, it is found that the frequency values for SA (AS) modes are higher than those for the cylinder with a hexagonal cross-section. The vibration frequencies for torsional modes (AA modes) are 7·0–8·0% higher than those of the hexagonal cylinder.

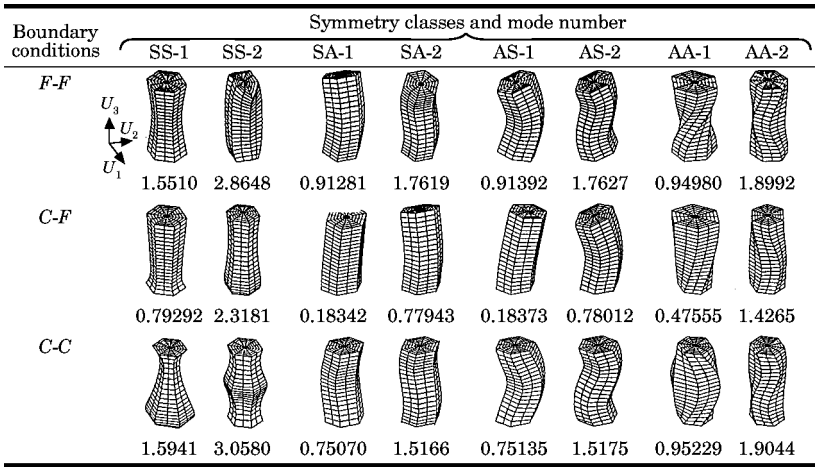

Figure 4. Vibration mode shapes of hexagonal cylinders subjected to different end support conditions ($L/a = 2{\cdot}0$, $\nu = 0{\cdot}3$, $\lambda = \omega a\sqrt{\rho/E}$).

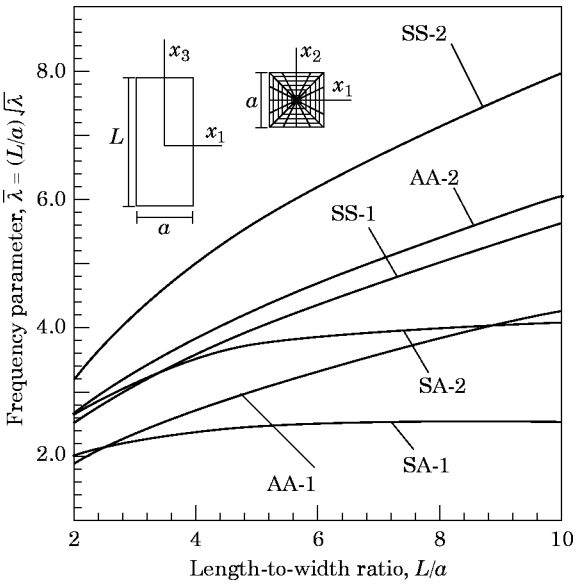

Figure 5. Plots of frequency parameters, $\bar{\lambda} = (L/a)\sqrt{\lambda}$, versus length-to-width ratio, L/a, for a square cylinder with stress free ends (*F-F*).

Plots of frequency parameters versus length-to-width ratio for elastic cylinders of square and hexagonal cross-sections are presented in Figures 5–10, respectively, for *F-F*, *C-F*, and *C-C* support conditions. To allow for direct comparison between different cross-sectional shapes, the width a is assumed to be the same for all shapes. The frequency parameter $\bar{\lambda}$ corresponds directly to the vibration frequency. In these plots, the first two frequencies corresponding to each symmetry class are presented. For the square cross-section,

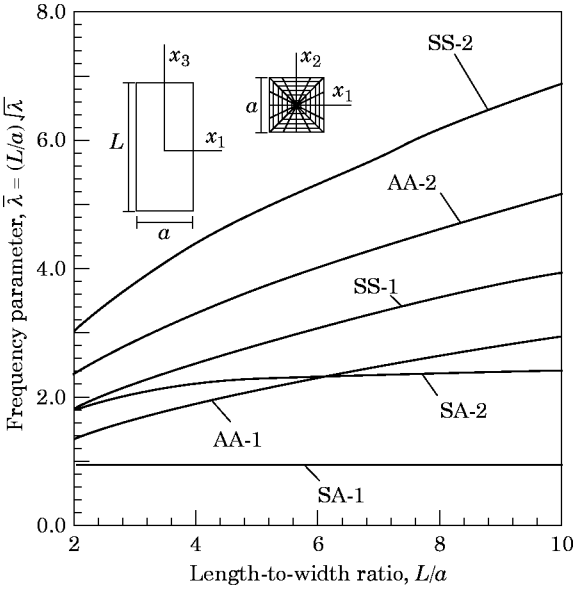

Figure 6. Plots of frequency parameters, $\bar{\lambda} = (L/a)\sqrt{\lambda}$, versus length-to-width ratio, L/a, for a square cylinder with cantilevered ends (*C-F*).

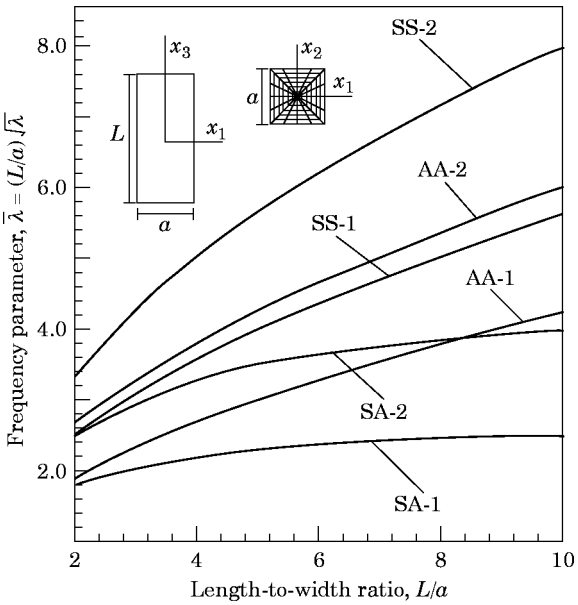

Figure 7. Plots of frequency parameters, $\bar{\lambda} = (L/a)\sqrt{\lambda}$, versus length-to-width ratio, L/a, for a square cylinder with clamped ends (C-C).

symmetry–antisymmetry (SA) and antisymmetry–symmetry (AS) modes possess identical frequencies. As to the effect of length-to-width ratio on the vibration frequency, it is observed that the frequency decreases monotonically as the length-to-width ratio increases. The decline is most steep for $L/a < 4{\cdot}0$. Beyond this range the vibration of frequency with L/a is more gradual and tends to converge asymptotically to the solution for an infinitely long beam.

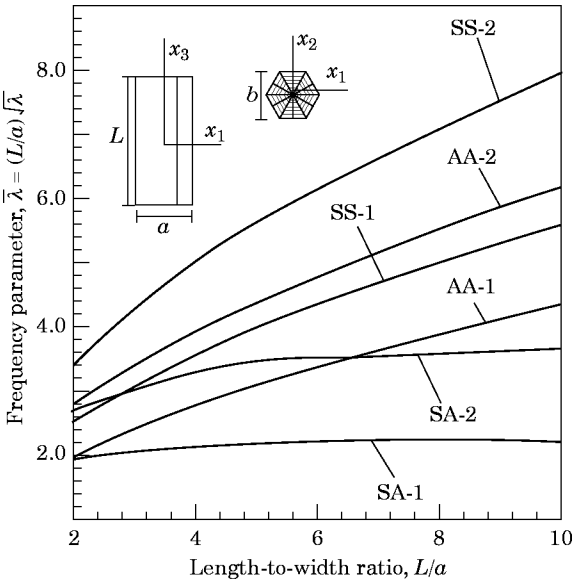

Figure 8. Plots of frequency parameters, $\bar{\lambda} = (L/a)\sqrt{\lambda}$, versus length-to-width ratio, L/a, for a regular hexagonal cylinder with stress free ends (F-F).

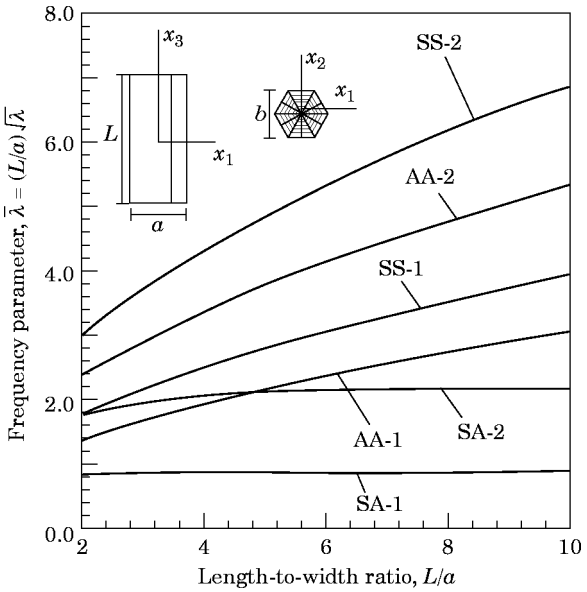

Figure 9. Plots of frequency parameters, $\bar{\lambda} = (L/a)\sqrt{\lambda}$, versus length-to-width ratio, L/a, for a regular hexagonal cylinder with cantilevered ends (C-F).

Several frequency crossings are evident in these plots. For instance, at length-to-width ratios $L/a < 3{\cdot}0$, the lowest vibration frequency for a F-F square cylinder corresponds to the AA-1 mode. At a higher length-to-width ratio, however, the flexural stiffness of transverse bending motion (AS-1) decreases rapidly and results in a frequency crossing with the AA-1 mode. Further frequency crossings at higher modes for the cylinder with a hexagonal cross-section are also evident. For cylinders with other boundary conditions, similar trends are also observed for the frequency spectra. Generally, it can be deduced

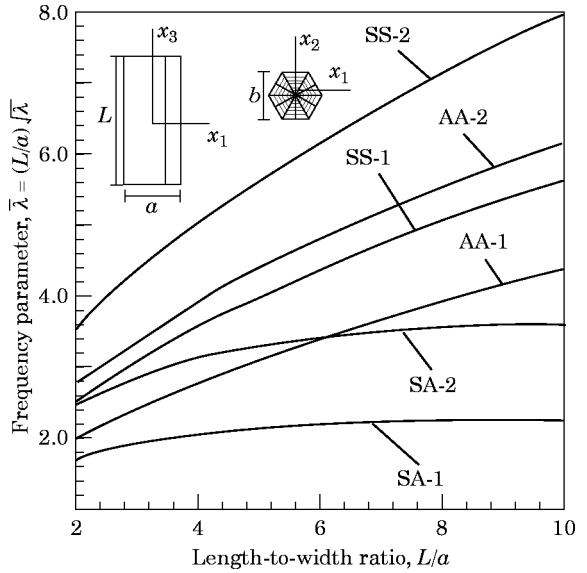

Figure 10. Plots of frequency parameters, $\bar{\lambda} = (L/a)\sqrt{\lambda}$, versus length-to-width ratio, L/a, for a regular hexagonal cylinder with clamped ends (C-C).

that, irrespective of the boundary conditions at both ends, the axial extensional (SS modes) motions always occur at a higher frequency of vibration.

5. CONCLUSIONS

A computational model, the *p*-Ritz method, for three-dimensional vibration analysis of elastic cylinders of polygonal cross-section has been developed on the basis of linear, small-strain, three-dimensional elasticity theory. The unique coupling of a two-dimensional lateral surface function with a one-dimensional longitudinal function allows the treatment of cylinders with a wide range of cross-sectional shapes and sizes. Extensive frequency results and vibration mode shapes have been presented in graphical forms. The effects of different end support conditions and the length-to-width ratios upon the natural vibration frequency of elastic cylinders of polygonal shape have been studied in detail. It is noted that the square cylinder possesses bending frequencies which are relatively higher than those of the hexagonal cylinder. However, the hexagonal cylinder has the highest torsional vibration frequency for all boundary conditions considered.

REFERENCES

1. S. P. Timoshenko 1921 *Philosophical Magazine* **41**, 744–746. On the correction for shear of the differential equation for transverse vibration of prismatic bars.
2. S. P. Timoshenko 1921 *Philosophical Magazine* **43**, 125–131. On the transverse vibration of bars of uniform cross-section.
3. J. R. Hutchinson 1981 *ASME Journal of Applied Mechanics* **48**, 581–585. Transverse vibration of beams, exact versus approximate solutions.
4. J. R. Hutchinson and S. D. Zillmer 1983 *ASME Journal of Applied Mechanics* **50**, 123–130. Vibration of a free rectangular parallelepiped.
5. J. R. Hutchinson and S. D. Zillimer 1986 *ASME Journal of Applied Mechanics* **53**, 39–44. On the transverse vibration of beams of rectangular cross-section.
6. A. W. Leissa and Z. D. Zhang 1983 *Journal of the Acoustical Society of America* **73**, 2013–2021. On the three-dimensional vibrations of the cantilevered rectangular parallelepiped.
7. K. M. Liew, K. C. Hung and M. K. Lim 1995 *ASME Journal of Applied Mechanics* **62**, 159–165. Free vibration studies on stress-free three-dimensional elastic solids.
8. K. M. Liew, K. C. Hung and M. K. Lim 1993 *International Journal of Solids and Structures* **30**, 3357–3379. A continuum three-dimensional vibration analysis of thick rectangular plates.
9. K. M. Liew, K. C. Hung and M. K. Lim 1994 *International Journal of Solids and Structures* **31**, 3233–3247. Three-dimensional vibration of rectangular plates: variance of simple support conditions and influence of in-plane inertia.
10. K. M. Liew, K. C. Hung and M. K. Lim 1995 *Journal of Sound and Vibration* **182**, 709–727. Three-dimensional vibration of rectangular plates: effects of thickness and edge constraints.